Metabolic Segregation and Characteristic Gene Clusters of the Key Functional Populations in Anaerobic Digestion Consortia

Yubo Wang[1,2], Ruoqun Zhang[1], Chunxiao Wang[2], Weifu Yan[2], Tong Zhang[2], Feng Ju[1]

Author Affiliation:

1. Institute of Advanced Technology, Westlake Institute for Advanced Study, Hangzhou 310024, Zhejiang Province, China

2.Environmental Microbiome Engineering and Biotechnology Laboratory, The University of Hong Kong, Pokfulam, Hong Kong

Abstract

Enrichment experiment integrated with genome-centric meta-omics analysis revealed function partition among populations in the three functional niches of the anaerobic digestion bioprocess: primary fermentation, secondary fermentation (syntrophic acetogenesis), hydrogenotrophic and acetoclastic methanogenesis. Accumulation of H_2 as a metabolic intermediate originates mainly from primary fermentation. Formate, rather than H_2, plays a key role in secondary fermentation, mediating interspecies electron transfer from the syntrophic oxidizing bacteria to the formate-utilizing methanogens. Both the flavin based electron bifurcating *HydABC* hydrogenase (Group A3 hydrogenase) and the ferredoxin-dependent GroupB hydrogenase are present and actively expressed in the primary fermenting bacteria, while both the cytosolic formate dehydrogenase and the membrane-bound formate dehydrogenase are absent in the primary fermenting bacteria; in comparison, the latter two types of formate dehydrogenase are present and actively transcribed in the secondary fermenting bacteria. Additionally, absence of the formate hydrogenlyase in both the primary fermenting bacteria and the secondary fermenting bacteria indicated limited interconversion of H_2 and formate in those strict anaerobic bacteria. Such segregation of the electron carrier pools by H_2 and formate in primary fermentation and in secondary fermentation, respectively, can benefit the syntrophic oxidizers with a higher tolerance to the accumulation of H_2 from the co-occurring primary fermentation. In addition, metabolic specificity and characteristic gene clusters are noted for anaerobes of the different function niches enriched in this study, i.e., primary fermenting bacteria *Clostridium* FI21,22, syntrophic butyrate oxidizer *Syntrophomoas* FI3,4,7, syntrophic propionate oxidizer *Smithellaceae* DES18-25, formate- and H_2-utilizing methanogen *Methanobacteriaceae* EA7, and acetoclastic methanogen *Methanothrix soehngenii* HA1,2,3.

Keywords: Anaerobic digestion, Enriched microbiota, Metabolic segregation, H_2 and formate, Genome-centric transcriptome, Characteristic gene clusters.

1. Introduction

Anaerobic digestion (AD) is of central importance in the field of environmental biotechnology since 1980s. It is one of the most cost-effective approaches to stabilize organic components in high-strength waste streams, aiding in bioenergy production and biosolids reduction [1-6]. However, challenges persist in addressing process upsets such as over-acidification and foam formation [7]. Fine-tuned control and optimization of the AD process depend on a deeper understanding of the sequential microbial reactions mediated by anaerobic populations across the four function niches: hydrolysis (conversion of polymers to monomers), primary fermentation/acidogenesis (conversion of monomers to H_2/HCOOH, acetate and other reduced fatty acids), secondary fermentation (conversion of reduced fatty acids to acetate and H_2/HCOOH) and methanogenesis (CH_4 generation mainly from acetate and H_2/HCOOH) [8-14].

Due to the limited amount of energy that can be harvested from the corresponding metabolism, secondary fermentation is often regarded as the bottleneck step in the AD bioprocess [15]. One of the objectives of this study is to chart the physiology of anaerobes in this specific function niche, specifically, syntrophic butyrate oxidizing bacteria (SBOBs) and syntrophic propionate oxidizing bacteria (SPOBs). As key intermediates in the anaerobic mineralization of organic compounds, propionate and butyrate can account for 20-43% of the total CH_4 formation [16].

One of the well-accepted metabolic traits of the SBOBs and the SPOBs is their thermodynamic sensitivity to H_2, with an estimated H_2 concentration at ~300 ppm being high enough to inhibit the anaerobic oxidation of propionate or butyrate[16]. In the established scheme of methanogenic carbon cycling, the metabolism of almost all substrates, such as carbohydrates and amino acids, generates H_2 [17, 18]. To our knowledge, there has been little systematic characterization on the dynamics (generation and turnover) of H_2 during the AD

bioprocess [19] and little evaluation has been conducted on the impact of H_2 accumulation as one of the fermentation byproducts on the co-occurring anaerobic oxidation of volatile fatty acids (VFAs) in the AD ecosystems [20-23]. Inhibition concentration of H_2 characterized at 2.03 kPa for anaerobic butyrate oxidation and at 11.1 kPa for anaerobic propionate oxidation are way much higher than the theoretical inhibition concentration of H_2 calculated at 300 ppm (~28 Pa) [19, 24, 25]. Additionally, evidence is accumulating that suggests formate plays a more important role than H_2 as an interspecies electron carrier in syntrophic oxidation [26, 27]. This study aims to address this knowledge gap by integrating the characterization of H_2 dynamics with the degradation dynamics of VFAs in lab-scale AD reactors.

Full-scale anaerobic digesters rarely harbor high numbers of syntrophic bacteria [5], although they do contain highly abundant primary fermenting populations. Given that syntrophic oxidation of reduced fatty acids proceeds at the thermodynamic limit of life [22, 28], another scientific question to be addressed in this study is: are the SBOBs and SPOBs obligate syntroph, or they more commonly are opportunists capable of fermentation flexibility [22, 29]? Many uncharacterized and uncultivated bacteria in the AD consortia have yet-to-be-identified relationships with the two trophic groups, i.e., primary fermentation *vs.* secondary fermentation, and an in-depth understanding on the metabolic flexibility or specificity of the syntrophic populations could help elucidate the intricate ecology that supports the methanogenic conversion of organic compounds.

To obtain consortia dominated by primary fermenting bacteria, SBOBs and SPOBs, enrichment experiment was conducted in this study with three sets of reactors, using glucose, butyrate and propionate as substrates, respectively. Metabolic versatility of the enriched anaerobes in the three function guilds was evaluated by their metabolic capacity towards and transcriptome response to either the fermentative substrates (i.e., glucose, fumarate, crotonate) or the reduced short-chain fatty acids (SCFAs, i.e., propionate, butyrate). Dynamics of the

generation and turnover of H_2 as an intermediate metabolite, and also the impact of H_2 accumulation on the syntrophic oxidation of propionate and butyrate, were monitored throughout the batch experiments.

2. Material and methods

2.1 Enrichment of primary fermenting bacteria, SBOBs and SPOBs

Three sets of AD consortia were enriched for the efficient methanogenic conversion of glucose, propionate and butyrate, respectively. Duplicate enrichments utilizing each substrate were processed in 1000-ml serum bottles with working volume of 500 ml. Hereafter, the consortia enriched with glucose as substrate will be referred to as 'Consortia-G', the consortia enriched with butyrate as substrate will be referred to as 'Consortia-B', and the consortia enriched with propionate as substrate will be referred to as 'Consortia-P'.

The inoculum used in this enrichment experiment was surplus sludge sampled from Chengxi wastewater treatment plant (Hangzhou, China). A detailed description on the seed sludge used, the feeding strategy, and methods for the physiochemical characterization of the biogas contents and the volatile fatty acids can be found in the supporting information.

2.2 Characterization on the metabolic flexibility of the primary fermenting bacteria, SBOBs and SPOBs

To characterize the metabolic flexibility of the primary fermenting bacteria, SBOBs and SPOBs, experiment was designed as summarized in Figure S2, to test the metabolic response of the enriched primary fermenting bacteria, SBOBs and SPOBs to different substrates applied. Take the test conducted on SBOBs enriched in Consortia-B as an example: after 219 days enrichment, the 1000 ml (500 ml *2) sludge from two parallel reactors of Consortia-B, in which SBOBs have been enriched, are combined and equally distributed into eight 200 ml serum bottles (each with a 125 ml working volume). In the subsequent batch tests, the primary substrate was sequentially switched from n-butyrate, to propionate, to glucose, to crotonate

(fumarate was applied for SPOBs in Consortia-P), and to the combined co-substrate mix of propionate:n-butyrate:glucose (COD:COD:COD=1:1:1). Degradation profile (Figure S3, S4, S5) of the varying substrates by the enriched SBOBs, and transcriptome response of the enriched SBOBs to the varying substrates applied was charted.

2.3 Biomass sampling, nucleic acid extraction, and meta-omics analysis

To profile the succession of the microbial community during the enrichment process, sludge samples were archived weekly or biweekly for sequencing-based analysis. Genomic DNA extracted from the seed sludge (day-0), and from sludge of the enriched consortia collected on day-85, day-134 and day-219 were subjected to metagenome sequencing. When metatranscriptome analysis is relevant, sludge samples (15 ml) collected at each time point were flash frozen in liquid nitrogen and stored in -80 ºC freezer prior to total RNA extraction. Metatranscriptome sequencing was conducted on 20 of the sludge samples collected in experiment described in section 2.2 (Table S1, Figure S3, S4, S5). A more detailed documentation on the genome-centric meta-omics analysis, the methodologies for 16S rRNA gene (v4-v5 region) based microbiome profiling, and the corresponding principal coordinate analysis (PCoA) are provided in the supporting information.

3. Results and discussion

3.1 Effects of glucose, butyrate and propionate on the succession of the anaerobic consortia enriched

Slow growth rates of the SBOBs and the SPOBs, and the selecting pressure imposed by SCFAs as the primary substrate is reflected by the significant decrease in the volatile suspended solids (VSS, a surrogate measure of the microbial biomass) in the Consortia-B and Consortia-P enriched. As summarized in Figure S6, at the same organic loading rate in terms of COD/L/d, in contrast to ~43% increment in VSS from 8.0 g/L to 11.7 g/l in Consortia-G, both Consortia-

B and Consortia-P are observed with a significant decrease in VSS by ~50% from 8.0 g/l to 4.1~4.4 g/l. Despite of the varying VSS contents, equally promising methanogenic conversion of glucose, butyrate and propionate is observed in the three consortia, i.e., Consortium-G, Consortia-B and Consortia-P, respectively (Figure S1).

A distinct shift in the composition of the microbiome is noted during the enrichment process. A detailed summary on the taxonomy affiliation of the top 15 genera and their relative abundance over the course of the enrichment can be found in Figure 1. Additionally summarized in Figure 2 is the PCoA analysis on the composition of the three consortia enriched. Over the course of the 219 days enrichment, genera that get characteristically enriched in Consortia-G are: *Clostridium sensu stricto3*, *Propionimicrobium* and an unclassified genus in the family of Propionibacteriaceae (g_un_f_Propionibacteriaceae). The one genus that gets characteristically enriched in Consortia-P is *Smithella*, and the one genus that gets characteristically enriched in Consortia-B is *Syntrophomonas*. Herein, we speculate that *Clostridium sensu stricto3*, *Propionimicrobium* and g_un_f_Propionibacteriaceae are primary fermenting bacteria utilizing glucose; *Smithella* is the putative SPOB oxidizing propionate anaerobically, and *Syntrophomonas* the putative SBOB oxidizing butyrate anaerobically.

As is summarized in Figure S7-a, after 219 days enrichment, the top 15 genera accounting for 75~83% of the populations in the three enriched consortia are of only ~4% relative abundance in the seed inoculum. Among these top 15 genera are two archaeal genera: *Methanosaeta* and *Methanobacterium*, and a much higher relative abundance of these two methanogen genera, especially *Methanobacterium* (Figure S7-b), is annotated in Consortia-B (20%) and Consortia-P (22%) than in Consortia-G (6%).

3.2 Genome-centric identification of the primary fermenting bacteria, SBOBs and SPOBs enriched

317 bacterial metagenome assembled genomes (MAGs) are recovered from the metagenome

datasets. A summary of their taxonomy affiliation, their relative abundance and their transcription activity can be found in Figure 3 and Appendix file 1. In the following genome-centric meta-omics analysis, we specifically focus on those 17 bacterial MAGs that have transcription response (>=0.5% of total mRNA clean reads mapped) to at least one of the substrates provided, i.e., glucose, propionate, butyrate, fumarate and crotonate. These 17 MAGs include FI21 and FI22 (hereafter, these two MAGs will be referred to as FI21, 22) affiliated to the genus of *Clostridium_T*; DES18, DES19, DES20, DES21, DES22, DES23, DES24, and DES25 (hereafter, these eight MAGs in the same genus of g_Fen_1166 will be referred to as DES18-25) affiliated to the family of *Smithellaceae*; FI3, FI4 and FI7 (hereafter, these three MAGs will be referred to as FI3,4,7) affiliated to the genus of *Syntrophomoas_B*; ER1, ER2 and ER4 (hereafter, these three MAGs will be referred to as ER1,2,4) that are annotatable only at the phylum level as *Eremiobacterota*; and TM1 affiliated to the species *Mesotoga*.

Considering that FI21,22 are among the populations that get specifically enriched with glucose as substrate in Consortia-G (datapoint G_DNA in Figure 3), DES18-25 enriched with propionate as substrate in Consortia-P (datapoint P_DNA in Figure 3) and FI3,4 with butyrate as substrate in Consortia-B (datapoint B_DNA in Figure 3), we tentatively assume that FI21, 22 are the primary fermenting bacteria utilizing glucose, FI3,4,7 are the SBOBs degrading butyrate, and DES18-25 are the SPOBs degrading propionate.

Further confirmed by the transcriptome analysis is the function niches of FI21, 22 as the primary fermenting bacteria, FI3,4,7 as SBOBs, and DES18-25 as SPOBs are. Specifically, when glucose is provided as the primary substrate to Consortia-G (datapoints gg2 in Figure 3), or as co-substrate to Consortia-B (datapoints bc4 in Figure 3) and Consortia-P (datapoints pc4 in Figure 3), FI21, 22 demonstrate the highest transcription activity in all the three consortia enriched, irrespective of their very low abundance in both Consortia-B and Consortia-P.

Consortia-G cannot use either butyrate or propionate efficiently, probably due to the extremely low abundance of the SBOB and SPOB populations in this community. When butyrate was provided as substrate to Consortia-B (datapoint bb4 in Figure 3) or to Consortia-P (datapoint pb5 in Figure 3), FI3,4,7 are noted with the highest transcription activity in both consortia. When propionate was provided as the primary substrate to either Consortia-B (datapoint bp5 in Figure 3) or Consortia-P (datapoint pp4 in Figure 3), consistent and relatively high transcription activity of DES18-25 is observed in both consortia.

The other four MAGs, ER1,2,4 and TM1, do not show consistent transcriptome response to the presence of any specific substrate tested, and they might be fermentative opportunists in the consortia, utilizing cell debris or other extracellular substances. A more detailed interpretation on the function niches of these four populations can be found in supporting information.

3.3 Transcription activity of the characteristic gene clusters mediating either flavin based electron bifurcation (FBEB) or reverse electron transfer (RET) in primary fermentation, in anaerobic butyrate oxidation and in anaerobic propionate oxidation

Transcription patterns of the key functional genes in bacterial MAGs of the three function niches are summarized in Figure 4. And summarized in Table 1 are the genes/gene clusters mediating either the flavin-based electron bifurcation (FBEB) or reverse electron transfer (RET) that are the featuring biochemistry in primary fermentation, in syntrophic butyrate oxidation and in syntrophic propionate oxidation.

3.3.1 The FBEB type hydABC gene cluster in primary fermenting bacteria and the non-FBEB type hydABC gene cluster in syntrophic oxidizing bacteria

High transcription activity of the cytosolic FBEB *HydABC* gene cluster in FI21,22 suggests the involvement of electron confurcation of Fd_{red} and NADH for H_2 generation during acetate generation (Figure 5a) in primary fermentation of the AD bioprocess where

hydrogenotrophic methanogens keep the H_2 concentration low.

The *hydABC* gene cluster is also annotated and with transcription activity in both SBOB *Syntrophomoas* FI3,4,7 and in SPOB *Smithelacea* DES18-25 (Figure 4). However, as is visualized in Figure 5, varying mutations are noted in the FMN-containing electron bifurcating subunit *hydB* in both *Syntrophomoas* FI3,4,7 and in *Smithelacea* DES18-25, comparing with that in the primary fermenting bacteria *Clostridium_T* FI21,22 enriched in this study and that in *Thermotoga maritima* MSB8 reference genome [30]. Among these mutations is a lack of the C-terminal end 2*[4Fe-4S] function domains as is also annotated in the *hydB* subunit of *S. aciditrophicus* [31] and of *S. wolfei* [32]. Biochemical characterization revealed that the activity of the FBEB-type *hydABC* H_2ase in *Thermotoga maritima* MSB8 requires the presence of both Fd_{red} and NADH (Reaction 'I' in Figure 5) [30], while enzyme products of the *hydABC* gene cluster in both *S. aciditrophicus* and *S. wolfei* cannot interact with Fdred and can use NADH as direct electron donor for the reduction of H^+ (Reaction 'ÍI' in Figure 5). Such shift in biochemistry mediated by the *hydABC* enzyme complex is probably a result of the mutations noted in its electron bifurcating *hydB* subunit [31, 32], and it also means that, recycling of the electron cofactor NAD^+ from NADH via the *hydABC* enzyme complex is thermodynamically more sensitive to H_2 accumulation in secondary fermentation than that mediated by the true FBEB-type *hydABC* in primary fermentation.

With similar mutations annotated in the *hydB* subunit as that in the biochemically characterized *hydABC* gene cluster in *S. aciditrophicus* and *S. wolfei*, we therefore interpret that the corresponding enzyme complex encoded by the *hydABC* gene cluster of both *Syntrophomoas* FI3,4,7 and of *Smithelacea* DES18-25 are also of the non-FBEB type, i.e., cannot interact with Fd_{red} and can use NADH as the direct electron donor for H^+ reduction and H_2 generation. And this NADH-coupled H^+ reduction is thermodynamically feasible only when the H_2 concentration is low enough (2.2 – 18.0 Pa) [31, 32] to sustain a higher electron potential

of the redox pair H^+/H_2 than that of the redox pair NAD^+/NADH (-280 mV) [33]. That is to say, in SBOB *Syntrophomoas* FI3,4,7 and SPOB *Smithelacea* DES18-25, the cytosolic recycling of NAD^+ via H^+ reduction will be inhibited under high H_2 concentrations, and NAD^+ need to be recycled with another electron acceptor rather than H^+, which is CO_2 reduction for formate generation during syntrophic oxidation of SCFAs.

3.3.2 Cytosolic and membrane-bound formate dehydrogenase in syntrophic oxidizing bacteria

Gene clusters encoding formate dehydrogenase (FDH) are uniquely annotated and identified with transcription activity in the secondary fermenting populations enriched in this study, i.e., SBOB *Syntrophomoas* FI3,4,7 and SPOB *Smithelacea* DES18-22. The cytosolic formate dehydrogenase (cFDH) catalyzes NADH-coupled HCO_3^-/CO_2 reduction and generate low concentrations of intracellular $HCOOH/HCOO^-$. The membrane-bound formate dehydrogenase (mFDH) catalyzes the proton motive force (PMF)-dependent reverse electron transfer (RET) of electrons from the membranous quinone (M)MKH_2 to CO_2, and generates low concentration of formate extracellularly. During syntrophic propionate and butyrate oxidation, low concentrations of formate maintained by both efficient interspecies formate transfer [34, 35] and by activity of the coupling formate-utilizing methanogen is essential for such formate-centered recycling of electron cofactors, NAD^+ and (M)MK^+ [36].

In comparison, neither cFDH nor mFDH is annotated in genomes of the primary fermenting bacteria *Clostridium* FI21,22 enriched in this study, therefore, formate is not relevant in the recycling of electron cofactors (Fd_{ox} or NAD^+) during primary fermentation. Formate as a fermentation product can originate from the activity of the pyruvate formate lyase (*PFL*), while transcriptional activity of *PFL* in *Clostridium* FI21,22 is much lower than that of pyruvate ferredoxin oxidoreductase (*PFOR*) as summarized in Figure 4. Altogether, the above genome-centric analysis and transcription activities of the key functional genes discussed

above suggests that H_2 is the dominant electron carrier in primary fermentation and formate is relevant more in secondary fermentation.

Formate hydrogenlyase (*FHL*) is not annotated or transcribed in either the primary fermenting populations or the secondary fermenting populations. Bacterial *FHL* can mediate the conversion of formate to H_2, and its absence suggests restricted biochemical interconversion of formate and H_2 in these strict anaerobic bacteria enriched in this study. In other words, metabolism of H_2 and formate as electron carriers in the anaerobic digestion bioprocess are segregated.

3.3.3 The cytosolic Bcd_EtfAB_H2ase gene cluster in primary fermenting bacteria and the membrane-bound Bcd_EtfAB_EMO gene cluster in syntrophic butyrate oxidizing bacteria

Butyryl-CoA dehydrogenase (*Bcd*) gene clustering with the electron transfer subunits *EtfA* and *EtfB* (hereafter, referred to as *Bcd_EtfAB*) is of high transcription activity in both the primary fermenting bacteria *Clostridium* FI21,22 and in the SBOB *Syntrophomoas* FI3,4,7.

In *Clostridium* FI21,22, *Bcd_EtfAB* neighbors with the GroupB ferredoxin-dependent [FeFe] hydrogenase (H_2ase). This *Bcd_EtfA1B1*_H_2ase gene cluster as a whole can mediate: 1) the NADH-dependent FBEB biochemistry of the crotonyl-CoA reduction to butyryl-CoA (Reaction 'b' in Table 1) [37], and 2) the succeeding H^+ reduction and H_2 production by the Fd_{red} generated (Reaction 'c' in Table 1) [38].

In contrast, a gene subunit encoding a membrane-bound oxidoreductase (*EMO*) is embedded in the *Bcd_EtfAB* gene cluster in genomes of the SBOB populations FI3,4,7. Unlike the *Bcd_EtfAB_H2ase* enzyme complex that is cytosolic, enzyme complex encoded by this *Bcd_EtfAB_EMO* gene cluster is membrane-bound and mediates one of the featuring biochemistry in anaerobic butyrate oxidation: the proton motive force (PMF)-dependent butyryl-CoA oxidation by the membranous methylmenaquinone (MMK) (Reaction 'b' in Table 1) [39]. The reduced form of $MMKH_2$ generated can further reduce CO_2 to formate, mediated

by the mFDH, which is the second PMF-dependent step in the anaerobic butyryl-CoA oxidation to crotonyl-CoA, and CO_2 in the terminal electron acceptor (Reaction 'e' in Table 1) [39].

3.3.4 Anaerobic succinate oxidation and the FdhB_mvhD_hdrABC gene cluster in syntrophic propionate oxidizing Smithellaceae

The SPOB populations, DES18-25, that get specifically enriched in this study are of a same undefined genus in the family of *Smithelacea.* Propionate conversion via the dismutation pathway, i.e., two propionate molecules being first converted to acetate and butyrate, and butyrate was then converted via β-oxidation, has been reported only in *Smithella propionica* [40, 41]. And methylmalonyl-CoA pathway is found in all other SPOBs characterized so far [5]. The SPOB DES18-25 enriched in this study is of the family *Smithelacea*, while resolution of the taxonomy assignment is not high enough to tell whether they are of *Smithella propionica* or not. As is summarized in Figure 4, both the presence and transcription activity of genes involved in the β-oxidation of butyrate and in the methylmalonyl-CoA pathway are observed in *Smithelacea* DES18-25.

One of the interesting transcription patterns noted in DES18-25 is of the *FdhB_MvhD_HdrABC* gene cluster. Transcription activity and proteome signal of the *FdhB_MvhD_HdrABC* gene cluster in SPOBs have been reported in previous studies [42, 43]. Bicohemical characterization of the *FdhAB_mvhD_HdrABC* enzyme complex in methanogens revealed their FBEB activity during methanogenesis from formate[36], while explicit biochemical evidence is absent regarding the catalytic activity of the *FdhB_MvhD_HdrABC* enzyme complex commonly annotated in SPOBs. Currently, there are two hypotheses regarding the function roles of this *FdhB_MvhD_HdrABC* gene cluster and the corresponding enzyme complex: it may either be involved in sulfate reduction[43] or may possess an uncharacterized FBEB activity [42]. We tentatively favor the second hypothesis for two reasons: 1) it was reported that the gram-negative bacteria *Smithella* cannot reduce sulfate [5], further,

in this study, to exclude the interference of sulfate as electron acceptor, we used a recently updated recipe for solution medium preparation [44], where $MgSO_4$ was replaced with $NaHCO_3$ (Supporting information); and 2) the *FdhB_MvhD_HdrABC* gene cluster showed high transcriptional activity almost exclusively under the presence of propionate as substrate. This is to say, we cannot exclude the possibility that this *FdhB_MvhD_HdrABC* enzyme complex is somehow relevant in mediating the anaerobic oxidation of succinate to fumarate, which is thermodynamically the most challenging step in anaerobic propionate oxidation *via* the methylmalonyl-CoA pathway [15].

3.4 Segregation of H_2 and formate metabolism in primary and secondary fermentation

As is discussed in the above section, in primary fermenting bacteria FI21,22, FBEB type *hydABC* and ferredoxin-dependent [FeFe] H_2ase, are annotated and transcribed, mediating electron transfer to H_2 during either acetate or butyrate fermentation, and no formate dehydrogenase (*FDH*) was annotated or transcribed. In contrast, uniquely transcribed with high activity in the secondary fermenting populations, i.e., SBOBs FI3,4,7 and SPOBs DES18-22, are *FDH*, medicating electron transfer from the membranous $MMKH_2$ or cytosolic NADH to CO_2 for formate generation. Interconversion of H_2 and formate is limited due to the absence of the FHL in both primary fermenting bacteria and in the syntrophic secondary fermenting bacteria.

One of the ecological relevance of such segregation of the H_2 and formate metabolism in the AD bioprocess could be that the 'H_2-tolerant' primary fermentation and the 'H_2-sensitive' secondary fermentation can proceed simultaneously, with H_2 being the electron carrier in the former, and formate as the predominant electron carrier in the latter. Under high concentrations of H_2 emitted from primary fermentation, the 'H_2-sensitive' secondary fermentation can proceed with formate as dominant electron carrier.

Our wet-lab observation aligns well with this hypothesis. Accumulation of H_2 in high

concentrations (5,000-70,000 ppm, Figure S8) was observed only when fermentative substances (i.e., glucose and fumarate) are present as either the only substrate or as co-substrate. H_2 accumulation was never detected when only either propionate or butyrate was supplied as the primary substrate.

Furthermore, if we assume that H_2 is the only electron carrier during secondary fermentation, the acetogenic oxidation of propionate and butyrate would become thermodynamically unfavorable when the gaseous H_2 content is above 132 ppm and 134 ppm, respectively[1] (Figure S9). In contrast to this theoretical calculation, when substrate mix as glucose:propionate:butyrate =1:1:1 (COD:COD:COD) was provided, intermittent H_2 accumulation to >30000 ppm was detected in both Consortia-B and Consortia-P, which was way much higher than the theoretical inhibition concentration of H_2 as calculated. And at the time points when such high H_2 concentrations were detected, the degradation of propionate and butyrate were not completely inhibited, as indicated by the decline of their concentrations summarized in Figure 6. As early as in 1980s, there have been reports on inhibition concentration of H_2 characterized at 2.03 kPa for anaerobic butyrate oxidation and at 11.1 kPa for anaerobic propionate oxidation [24, 25], however, till now, results of these two studies have been largely overlooked and no follow-up work has been conducted to elaborate why the anaerobic oxidation of propionate and butyrate can proceed at such high H_2 concentrations.

Formate being the dominant interspecies electron carrier during syntrophic oxidation, and the absence of biochemistry for H_2 conversion to formate, can be the two reasons why butyrate and propionate oxidation can proceed under high concentration of H_2 emitted from the co-occurring primary fermentation. Although high transcription activity of *FDH* was noted in SBOBs and SPOBs, we did not measure significant accumulation of formate during either

[1] Calculated at pH=7.0±0.5, (35±1) °C, acetate, propionate and butyrate concentration at 10 mM, CH_4 and CO_2 content in the gaseous phase at 70% and 30%.

butyrate or propionate degradation. Formate concentration below the detection limit (1 mM) is probably due to rapid interspecies formate transfer [34] and efficient utilization of formate by the coupling methanogens in the consortia enriched [36].

3.5 Formate- and H_2-utilizing methanogen and acetoclastic methanogen identified in the enriched consortia

Among the 39 archaeal MAGs recovered (Figure 7), 4 archaeal MAGs are of the highest transcriptional activity, accounting for (79±9) % of the mRNA gene transcripts mapped to the 39 archaeal MAGs. These 4 archaeal MAGs are: EA7 affiliated with the family of *Methanobacteriaceae*, and HA1, HA2, HA3 (hereafter, termed as HA1,2,3) affiliated with the species of *Methanothrix soehngenii*. In the following genome-centric interrogation, we focused specifically on these 4 archaeal MAGs, to elaborate on the methanogenic activity of the enriched consortia.

According to the transcription profile as summarized in Figure 8 and Figure S10, EA7 is a formate- and H_2- utilizing methanogen and HA1,2,3 are acetoclastic methanogens. Specifically, *Methanobacteriaceae* EA7 dominated the transcription activity of genes encoding Formate dehydrogenase (coenzyme F420-coupled, denotated as *FdhAB*), formylmethanofuran dehydrogenase (*fwd*), and coenzyme F420 hydrogenase (*frh*). In comparison, *Methanothrix soehngenii* HA1,2,3 dominated the mRNA transcripts of genes encoding the acetyl-CoA decarbonylase (*cdhDE*) and the carbon-monoxide dehydrogenase (*cdhAB*). The acetoclastic archaeal MAGs HA1,2,3 are of high identity to strain *Methanothrix soehngenii*, while the hydrogenotrophic archaeal MAG EA7 are annotatable only at the family level of *Methanobacteriacea,* indicating novelty of this hydrogenotrophic methanogen population enriched.

Formate as an important electron carrier in the syntrophic cooperation between the SBOB/SPOB and the methanogen archaea is hinted also by the high transcription activity, in

EA7, of the *fdhC* gene encoding formate transporter, and also the presence and the high transcription activity of the *FdhAB_mvhD_HdrABC* gene cluster. The formate-centered FEBE biochemistry mediated by this *FdhAB_mvhD_hdrABC* enzyme complex is reaction (1). Also annotated in EA7 is the presence and transcription activity of the *MvhAG_MvhD_HdrABC* gene cluster, mediating the H_2-centered FBEB reaction (2). Both *MvhAG_MvhD_HdrABC* and *FdhAB_mvhD_hdrABC* can couple the first step and last step of wolf cycle in methanogenesis [45].

$$2HCOOH + Fd_{ox} + CoM\text{-}S\text{-}S\text{-}CoB = 2H^+ + 2CO_2 + Fd_{red} + CoM\text{-}SH + CoB\text{-}SH \quad (1)$$

$$2H_2 + Fd_{ox} + CoM\text{-}S\text{-}S\text{-}CoB = 2H^+ + Fd_{red} + CoM\text{-}SH + CoB\text{-}SH \quad (2)$$

3.6 Metabolic specificity of the key functional populations in the AD consortia

According to characterization of the three AD consortia enriched in this study, there is a clear function partition of the primary fermentation, syntrophic butyrate oxidation, syntrophic propionate oxidation, hydrogenotrophic methanogenesis, and acetoclastic methanogenesis into distinct anaerobe populations. And such partition could be clearly seen in Figure 9 that schematically assigned the characteristic gene clusters underlying the featuring biochemistry to the corresponding anaerobe populations. In whichever of the three consortia enriched, when butyrate was provided as the primary substrate or as a co-substrate, (100±0) % of the *EMO* gene transcripts in the *Bcd_etfAB_EMO* gene cluster were expressed by the SBOBs. When propionate was provided as the primary substrate or as a co-substrate, (90±5)% of the Succinate dehydrogenase (*Sdh)* gene transcripts were expressed by the SPOBs. When glucose was provided as the primary substrate or as a co-substrate, the primary fermenting populations contributed (97±2)% of the transcripts of genes involved in the glycolysis &fermentation metabolism, e.g., the *PFOR* gene.

cFDH and *mFDH* were exclusively annotated and transcribed in syntrophic populations (SBOBs FI3,4,7 and SPOBs DES18-22). Coenzyme F420-dependent formate dehydrogenase

(*FdhAB*) exclusively in the hydrogenotrophic methanogen EA7. This again highlighted formate as the electron carrier between syntrophic oxidizers and hydrogenotrophic methanogens.

The acetoclastic methanogens *Methanothrix* HA1,2,3 and the hydrogenotrophic *Methanobacteriacea* EA7 equally dominant the overall CH_4 generation, as these two groups of methanogens each contributed ~50% of the Methyl coenzyme M reductase (*mcrA*) gene transcripts. The *Methanobacteriaceae* EA7 dominated methanogenic conversion of formate and H_2 by contributing (95±2) % of the transcripts of the functional genes, e.g., *frhA*, *fdhC* genes. The *Methanothrix soehngenii* HA1,2,3 dominated methanogenic conversion of acetate by contributing (92±4) % of the transcripts of functional genes, e.g., the *cdhA* gene.

We also tried to evaluate the metabolic flexibility of SBOB and SPOB by their ability to utilized either crotonate or fumarate. At the community level, both crotonate fermentation for butyrate generation in Consortia-B (Figure S3) and fumarate fermentation for propionate generation (Figure S4) in Consortia-P were detected after a long lag phase of 40-50 hours. However, due to the low transcription activity of both FI3,4,7 and DES18-25 to the fermentative substrates (denotated as S3 in Figure 4) provided, we cannot derive the conclusion that the SBOB or SPOB are the responsible populations for this crotonate or fumarate fermentation, by reversing the syntrophic oxidation of butyryl-CoA or succinate. In other words, the *Syntrophomonas_B* SBOB FI3,4,7 and the *Smithellaceae* SPOB DES18-25 enriched in this study are of limited metabolic flexibility in utilizing either crotonate or butyrate and gain energy via fermentation.

Conclusions

Revealed in this study is the segregation of H_2- and formate-metabolism in anaerobic digestion bioprocess, with H_2 being dominant as electron carrier in primary fermentation, and formate being dominant in the co-occurring secondary fermentation. No biochemistry is available for the interconversion of H_2 and formate, such segregation benefit the anaerobic oxidation of

butyrate and propionate with higher tolerance to H_2 accumulated as metabolic intermediate from primary fermentation.

Apart from the metabolic segregation of the H_2 metabolism and HCOOH metabolism in AD bioprocess, metabolic segregation is also noted among key function niches in the AD consortia, i.e., primary fermentation, syntrophic butyrate oxidation, syntrophic propionate oxidation, H_2- and formate-utilizing methanogenesis, and acetoclastic methanogenesis. Metabolic specificity rather than metabolic flexibility is ruling the AD ecosystem. Genome-centric transcriptome analysis integrated with wet-lab activity test revealed several characteristic gene clusters mediating the featuring biochemistry of each function niche listed above, which can further enable the genotype-phenotype correlation. Specifically, *FEBE hydABC* and *Bcd_etfAB_H$_2$ase* in *Clostridium_T*, the primary fermenting bacteria; *Bcd_etfAB_EMO* in the syntrophic butyrate-oxidizing bacteria (SBOB) in the genus of *Syntrophomonas_B*, *Sdh* and *FdhB_mvhD_hdrABC* in the syntrophic propionate-oxidizing bacteria (SPOB) affiliated to *Smithellaceae*, *FdhC_FdhAB_mvhD_hdrABC* and *mvhABG_mvhD_hdrABC* in the one hydrogenotrophic methanogen affiliated to *Methanobacteriaceae*, and *cdhA* in the acetoclastic methanogen species *Methanothrix soehngenii*. *cFDH* and *mFDH* are present and with high transcription activity only in SBOB and SPOB, and *FdhAB* only in hydrogenotrophic *Methanobacteriaceae*. Both the *Syntrophomonas_B* SBOB and the *Smithellaceae* SPOB enriched in this study are of limited fermentation flexibility in utilizing either crotonate or fumarate for butyrate and propionate generation, respectively.

Comparing with that in the primary fermenting bacteria *Clostridium_T* FI21,22, mutations in the *hydB* subunit are noted in the *hydABC* gene cluster of both *Syntrophomonas_B* SBOB and *Smithellaceae* SPOB. Such mutations can render a shift in the biochemistry mediated by the *hydABC* enzyme complex. Specifically, the *hydABC* enzyme complex in SBOB and SPOB

can interact with NADH as direct electron donor for H^+ reduction. While the *hydABC* enzyme complex in the primary fermenting bacteria are of true FBEB activity, cannot interact with either NADH or Fd_{red} alone, and need the presence of both NADH and Fd_{red} for H^+ reduction.

Taken together, our work provides new insights into interspecies electron transfer in the AD bioprocess, the metabolism of H_2 and HCOOH as electron carrier are segregated. Moreover, interrogation at the gene cluster level and the several characteristic gene clusters identified demonstrate an approach that will pave the way for improved genome-centric genotype-phenotype correlation for strict anaerobes that are elusive to be isolated as pure cultures for physiological characterization.

Data Availability Statement

Metagenome DNA (10 datasets in total) and metatranscriptome RNA (20 data sets in total) sequencing data are available in the NCBI Sequence Read Achieve (SRA) database under the Bioproject accession number of PRJNA886957. The 17 bacterial MAGs and 4 archaeal MAGs analyzed in this study are accessible in NCBI under the Bioproject accession number of PRJNA886046, function genes annotated in these 21 MAGs and their transcription activity could be found in Appendix file 1. 16S rRNA gene amplicon sequences (v4-v5 region) have also been deposited in NCBI under the Bioproject accession number of PRJNA885972.

Declaration of Competing Interest

The authors declare that there is no competing interest.

Abbreviations

SBOBs - syntrophic butyrate oxidizing bacteria; SPOBs - syntrophic propionate oxidizing bacteria; AD - anaerobic digestion; VFAs - volatile fatty acids; SCFAs - short-chain fatty acids; COD - chemical oxygen demand; PCoA - principle coordinate analysis; VSS - volatile suspended solids; MAGs - metagenome assembled genomes; FBEB – flavin based electron bifurcation; RET – reverse electron transfer; PMF – proton motive force; PFL – pyruvate

formate lyase; PFOR – pyruvate ferredoxin oxidoreductase; FHL – formate hydrogenlyase; EMO – membrane-bound oxidoreductase.

Acknowledgments

This work was supported by the Zhejiang Provincial Natural Science Foundation of China under Grant No. LR22D010001 and Key R&D Program of Zhejiang (2022C03075) and Research Center for Industries of the Future (RCIF). Technical assistance from Ms. Yisong Xu in laboratory affairs and Mr. Guoqing Zhang in maintaining the in-house computing facility are greatly appreciated.

Authors' contributions

YW conceptualized this research and discussed with FJ. YW conducted the wet-lab experiment, the meta-omics data analysis and visualization, and wrote the manuscript. RZ participated in the wet-lab experiment. CW, WY, TZ and FJ participated in proof reading and revision of the manuscript. FJ acquired funding for this research.

1 **Table1.** Presence (+) and absence(-) of the gene clusters mediating either flavin based electron bifurcation (FBEB) or reverse electron transfer
2 (RET) in primary fermentation and in syntrophic oxidation of butyrate and propionate, their cellular component and the corresponding
3 biochemistry

Gene/ Gene clusters	**Cellular component**	**Biochemical reaction**	**Primary fermenting bacteria**	**SBOB**	**SPOB**
			FI21,22	FI3,4,7	DES18-25
hydA_hydB_hydC	Cytoplasm	a.1) Fd_{red} + NADH + $4H^+$= $2H_2$ + NAD^+ + Fd_{ox} (in primary fermentation); a.2) NADH + $2H^+$ = H_2 + NAD^+ (in syntrophic oxidation)	+	+	+
Bcd_EtfA_EtfB_H₂ase	Cytoplasm	b) 2NADH + Crotonyl-CoA + Fd_{ox} = 2 NAD^+ + Butyryl-CoA + Fd_{red}	+	-	-
cFDH	Cytoplasm	c) NADH + CO_2 + H^+ = NAD^+ + HCOOH	-	+	+
mFDH	Membrane-bound	d) (M)MKH_2 + CO_2 + PMF = HCOOH + (M)MK	-	+	+
FdhB_mvhD_HdrABC	Cytoplasm	UNKNOWN	-	-	+
Bcd_EtfB_EMO_EtfA	Membrane-bound	e) Butyryl-CoA + MMK + PMF = Crotonyl-CoA + $MMKH_2$	-	+	-
SdhA_SdhB_SdhC	Membrane-bound	Succinate + (M)MK+ PMF = Fumarate + (M)MKH_2	-	-	+

4

Figure list

Figure 1. Taxonomy affiliation and relative abundance of the top 15 genus in the three consortia enriched with glucose, propionate and butyrate, respectively. Summarized in this figure are the 16S rRNA gene (v4-v5 region) based microbiome profile in Consortia-G, Consortia-B and Consortia-P from day 37 to day 219, and in seed sludge on day 0.

Figure 2. Principal coordinates analysis (PCoA) of the three anaerobic digestion consortia enriched with glucose, propionate and butyrate, respectively. The community structures were inferred from the 16S rRNA amplicon sequence variants (v4-v5 region), and the PCoA analysis is based on the euclidean distance matrix. PCoA1 and PCoA2 are shown with the percentage variation explained by each axis. During the course of the 219 days enrichment, the most varying population in Consortia-G were genus *Clostridium sensu stricto* 3, *Propionimicrobium*, and an unclassified genus in the family of *Propionibacteriacea*; the most varying population in Consortia-P was the genus *Smithella*, and the most varying population in Consortia-B was the genus *Syntrophomonas*.

Figure 3. Maximum likelihood tree of the 315 bacterial MAGs recovered in this study. The inner heatmap summarized the meta-DNA based abundance and the meta-RNA based transcription activity of each MAG. 'seed_DNA', 'B_DNA', 'P_DNA' and 'G_DNA' denoted meta-DNA based abundance of each MAG in the seed sludge, in the enriched Consortia-G, Consortia-B and Consortia-P, respectively. The other datapoints are the meta-RNA based transcription activity of each MAG. A detailed information on each datapoint for meta-RNA based transcription analysis could be found in Table S1 and Figure S3-S5. The 17 MAGs highlighted with white bold labels were those MAGs annotated with relatively high transcription activity in response to certain substrates provided. This phylogenetic tree was constructed using FastTree [46] (maximum-likelihood phylogeny) based on a set of 120 concatenated universal single-copy proteins for Bacteria [47]. Branches of the phylogenetic tree are coloured according to their taxonomy affiliation at the phylum level, and those grey dots at each inner node indicate bootstrap values >=0.9.

Figure 4. Variations in the transcription activity of the key functional genes annotated in the 17 MAGs in response to the stimuli of varying substrates in A) Consortia-B, B) Consortia-P and C) Consortia-G. FI3,4,7 refers to the three SBOB in the genera of *Syntrophomonas_B*, DES18-25 refers to the eight SPOB of a same unnamed genera in the family of Smithellaceae, FI21,22 refers to the two parimary fermenting bacteria in the genera of *Clostridium_T*, TM1 refers to the one *Mesotoga* MAG, and ER1,2,4 refers to the 3 co-occurring *Eremiobacterota* MAGs. S1, S2 and S3 listed horizontally denotated substrate as n-butyrate, propionate and fermentative substrate, respectively. The fermentative substrate applied is glucose in Consortia-G, fumarate in Consortia-P and crotonate in Consortia-B. Sc denoted substrate mix as glucose: propionate: butyrate=1:1:1 (COD:COD:COD). ScH_2 and $S3H_2$ refer to the datapoints when there is accumulation of H_2, when fermentative substrate is present or substrate mix is applied. Colors of the circles indicate changes in the transcription activity of the corresponding genes, in log difference relative to that of datapoint g0, b0 and p0 where no substrate is available at the end of an SBR batch. Size of the circles indicate the square root of the RNA-RPKM values of the corresponding genes. Clustered in M01 are key genes involved in butyrate oxidation, in M02 are key genes involved in propionate oxidation, in M03 are key genes involved in the glycolysis and pyruvate metabolism, in M04 are key genes involved in the fatty acid synthesis, in M05 are the cytosolic and membrane-bound formate dehydrogenase, in M06 are hydrogenase genes, in M07 are genes encoding the electron transfer flavoprotein. For clarity,

the *EtfA* and *EtfB* subunits in the *Bcd_EtfAB_H₂ase* gene cluster are denoted as *EtfA1* and *EtfB1*, while *EtfA* and *EtfB* subunits in the *Bcd_EtfAB_EMO* gene cluster are denoted as *EtfA2* and *EtfB2*. In M08 is the ATP synthase gene, in M09 are genes encoding the type IV pili, flagellar and fimbria assembly protein, in M10 are genes encoding the protease, murein-degrading enzymes and amylase etc., in M11 are genes encoding the synthesis of protein, amino acids, and glycogen. Full names of those genes denoted with abbreviations could be found in the Appendix file 1.

Figure 5. Summary of the C-terminal end domain in the *hydB* subunit in the flavin based electron bifrucation (FBEB) type of *hydABC* in the primary fermenting populations (upper box) and in the non-FBEB type *hydABC* in the SBOB and SPOB. Name of the reference microbe strains in which the catalytic activity of the corresponding *hydABC* enzyme complex has been characterized are highlighted in blue. Names of the anaerobe populations enriched in study are shown in grey. Provided in the brackets are the gene accession number of the corresponding *hydB* gene.

Figure 6. Degradation profile of propionate (HPr) and butyrate (HBut), and dynamics of H_2 concentration when substrate mix as glucose:propionate:butyrate = 1:1:1 (COD:COD:COD) was provided as substrate in a) Consortia-P, b) Consortia-B, and c) Consortia-G. d) Gibbs free energy change calculated for the degradation of propionate, n-butyrate and iso-butyrate in Consortia-P and Consortia-B , respectively, assuming that H_2 is the only electron carrier generated from the syntrophic oxidation of butyrate or propionate.

Figure 7. Maximum likelihood tree of the 39 archaeal MAGs recovered in this study. The inner heatmap summarized the meta-RNA based transcription activity of each MAG. A detailed information on each meta-RNA datapoint could be found in Table S1. The tree was constructed using FastTree (maximum-likelihood phylogeny) [46] based on a set of 122 concatenated universal single-copy proteins for *Archaea* [47]. Branches of the phylogenetic tree are coloured according to their taxonomy affiliation, and those light purple dots indicate bootstrap values >=0.9.

Figure 8. Transcription activity of the key functional genes annotated in the Methanobacteriaceae MAG EA7, and in the three *Methanothrix* MAGs HA1,2,3. The heatmap represents the transcription activity of the corresponding genes, and the data given alongside the heatmap bar are square root of the RNA-RPKM values. Full names of genes denoted with abbreviations could be found in the Appendix file 1. Genes grouped in grid R1 are those specifically involved in acetoclastic methanogenesis, genes grouped in grid R2.1-R2.3 are those specifically involved in hydrogenotrophic methanogenesis, and genes grouped in grid R3 are genes shared by both the hydrogenotrophic methanogenesis and acetoclastic methanogenesis

Figure 9. Contribution of the putative fermenter bacteria *Clostridium_T* FI21,22, the SBOB *Syntrophomonadaceae* FI3,4,7), the SPOB *Smithellaceae*, DES18-25 to the mRNA transcripts of the core genes (left, coloured by genes) involved in the butyrate metabolism (*EMO, membrane-bound oxidoreductase clustering with Bcd_EtfAB*), the propionate metabolism (*Sdh*, Succinate dehydrogenase) and the pyruvate fermentation (*PFOR,* Pyruvate-ferredoxin oxidoreductase), in response to the availability of butyrate, propionate and glucose, respectively. And also, contribution of *Methanobacteriaceae* EA7 and *Methanothrix_soehngenii* HA1,2,3 to the mRNA transcripts of the core genes involved in the methanogenesis metabolism, i.e., *fdhA*: formate dehydrogenase (coenzyme F420) alpha subunit, *fdhC*: formate transporter, *cdhA*: acetyl-CoA decarbonylase, and *mcrA*: methyl coenzyme M reductase. Colours represent different genes, and the width of each ribbon represents the contribution ratios of each microbe group to the mRNA transcripts of each gene, the ratios were averaged across the transcription activity of the corresponding populations in the three enriched consortia: Consortia-G, Consortia-B and Consortia-P. *cFDH* and *mFDH*

101 refer to the cytosolic and membrane-bound formate dehydrogenase, respectively.

References

1. Ariesyady, H.D., T. Ito, and S. Okabe, *Functional bacterial and archaeal community structures of major trophic groups in a full-scale anaerobic sludge digester.* Water Res, 2007. **41**(7): p. 1554-68.
2. Bryant, R.I.M.a.M.P., *Metabolic Activity of Fatty Acid-Oxidizing Bacteria and the Contribution of Acetate, Propionate, Butyrate, and CO_2 to Methanogenesis in Cattle Waster at 40 and 60^0C.* Appl Environ Microbiol, 1981. **41**: p. 1363-1373.
3. Jain, M., *Anaerobic Membrane Bioreactor as Highly Efficient and Reliable Technology for Wastewater Treatment—A Review.* Advances in Chemical Engineering and Science, 2018. **08**(02): p. 82-100.
4. Speece, R.E., *Anaerobic biotechnology for industrial wastewater treatment.* Environ Sci Technol, 1983. **17**(9): p. 416A-27A.
5. Stams, A.J., et al., *Role of syntrophic microbial communities in high-rate methanogenic bioreactors.* Water Sci Technol, 2012. **66**(2): p. 352-62.
6. Macarie, H., *Overview of the application of anaerobic treatment to chemical and petrochemical wastewaters.* Water Sci Technol, 2000. **42**(5-6): p. 201-214.
7. Moeller, L. and A. Zehnsdorf, *Process upsets in a full-scale anaerobic digestion bioreactor: over-acidification and foam formation during biogas production.* Energy, Sustainability and Society, 2016. **6**(1).
8. Schink, B., *Energetics of Syntrophic Cooperation in Methanogenic Degradation.* Microbiology and Molecular Biology Reviews, 1997. **61**: p. 262-280.
9. Rudolf K. Thauer, K.J., and Karl Decker, *Energy Conservation in Chemotrophic Anaerobic Bacteria.* Bacteriol Rev, 1977. **41**: p. 100-180.
10. Michael J. McInerney, M.P.B., and Norbert Pfennig, *Anaerobic Bacterium that Degrades Fatty Acids in Syntrophic Association with Methanogens.* Arch Microbiol, 1979. **122**: p. 129-135.
11. Nobu, M.K., et al., *Microbial dark matter ecogenomics reveals complex synergistic networks in a methanogenic bioreactor.* ISME J, 2015. **9**(8): p. 1710-22.
12. Narihiro, T., et al., *The nexus of syntrophy-associated microbiota in anaerobic digestion revealed by long-term enrichment and community survey.* Environ Microbiol, 2015. **17**(5): p. 1707-20.
13. McInerney, M.J., et al., *Physiology, ecology, phylogeny, and genomics of microorganisms capable of syntrophic metabolism.* Ann N Y Acad Sci, 2008. **1125**: p. 58-72.

14. C. Adinarayana Reddy, M.P.B., and M. J. Wolin, *Characteristics of S Organism Isolated from Methanobacillus omelianskii.* Journal of Bacteriology, 1972. **109**: p. 539-545.
15. Westerholm, M., M. Calusinska, and J. Dolfing, *Syntrophic propionate-oxidizing bacteria in methanogenic systems.* FEMS Microbiol Rev, 2022. **46**(2).
16. Nobu, M.K., et al., *Catabolism and interactions of uncultured organisms shaped by eco-thermodynamics in methanogenic bioprocesses.* Microbiome, 2020. **8**(1): p. 111.
17. Paskins, L.J.C.a.A.R., *Measurement of Trace Concentrations of Hydrogen in Biogas from Anaerobic Digesters Using an Exhaled Hydrogen Monitor.* Water Res, 1987. **21**: p. 1567-1572.
18. de Kok, S., et al., *Impact of dissolved hydrogen partial pressure on mixed culture fermentations.* Appl Microbiol Biotechnol, 2013. **97**(6): p. 2617-25.
19. Birgitte K. Ahring, P.W., *Kinetics of Butyrate, Acetate, and Hydrogen Metabolism in a Thermophilic, Anaerobic, Butyrate-Degrading Triculture.* Appl Environ Microbiol, 1987. **53**: p. 434-439.
20. R. Conrad, B.S., and T.J. Phelps, *Thermodynamics of H_2-consuming and H2-producing metabolic reactions in diverse methanogenic environments under in situ conditions.* FEMS Microbiol Eco, 1986. **38**: p. 353-360.
21. Sieber, J.R., et al., *The genome of Syntrophomonas wolfei: new insights into syntrophic metabolism and biohydrogen production.* Environ Microbiol, 2010. **12**(8): p. 2289-301.
22. Sieber, J.R., M.J. McInerney, and R.P. Gunsalus, *Genomic insights into syntrophy: the paradigm for anaerobic metabolic cooperation.* Annu Rev Microbiol, 2012. **66**: p. 429-52.
23. R. Conrad, B.S., and T.J. Phelps *Thermodynamics of H2-consuming and H2-producing metabolic reactions in diverse methanogenic environments under in situ conditions* FEMS Microbiology Ecology, 1986. **38**: p. 353-360.
24. Ahring, B.K., *Product Inhibition of Butyrate Metabolism by Acetate and Hydrogen in a Thermophilic Coculture.* APPLIED AND ENVIRONMENTAL MICROBIOLOGY, 1988. **54**: p. 2393-2397.
25. Satoshi Fukuzaki, N.N., Manabu Shobayashi, and Shiro Nagai, *Inhibition of the Fermentation of Propionate to Methane by Hydrogen, Acetate, and Propionate.* Appl Environ Microbiol, 1990. **1990**: p. 719-723.
26. Leslie A. Day, E.L.K., Dallas R. Fonseca, Kyle C. Costa, *Interspecies Formate Exchange Drives Syntrophic Growth of Syntrophotalea carbinolica and Methanococcus maripaludis.* Appl Environ Microbiol, 2022. **88**.
27. de Bok, F.A., M.L. Luijten, and A.J. Stams, *Biochemical evidence for formate*

transfer in syntrophic propionate-oxidizing cocultures of Syntrophobacter fumaroxidans and Methanospirillum hungatei. Appl Environ Microbiol, 2002. **68**(9): p. 4247-52.

28. Kleerebezem, R. and A.J.M. Stams, *Kinetics of syntrophic cultures: A theoretical treatise on butyrate fermentation.* Biotechnology and Bioengineering, 2000. **67**(5): p. 529-543.
29. Worm, P., et al., *A genomic view on syntrophic versus non-syntrophic lifestyle in anaerobic fatty acid degrading communities.* Biochim Biophys Acta, 2014. **1837**(12): p. 2004-2016.
30. Schut, G.J. and M.W. Adams, *The iron-hydrogenase of Thermotoga maritima utilizes ferredoxin and NADH synergistically: a new perspective on anaerobic hydrogen production.* J Bacteriol, 2009. **191**(13): p. 4451-7.
31. Losey, N.A., et al., *The Beta Subunit of Non-bifurcating NADH-Dependent [FeFe]-Hydrogenases Differs From Those of Multimeric Electron-Bifurcating [FeFe]-Hydrogenases.* Front Microbiol, 2020. **11**: p. 1109.
32. Losey, N.A., et al., *Syntrophomonas wolfei Uses an NADH-Dependent, Ferredoxin-Independent [FeFe]-Hydrogenase To Reoxidize NADH.* Appl Environ Microbiol, 2017. **83**(20).
33. Buckel, W. and R.K. Thauer, *Flavin-Based Electron Bifurcation, A New Mechanism of Biological Energy Coupling.* Chem Rev, 2018. **118**(7): p. 3862-3886.
34. David R. Boone, R.L.J., and Yitai Liu, *Diffusion of the Interspecies Electron Carriers H2 and Formate in Methanogenic Ecosystems and Its Implications in the Measurement of Km for H2 or Formate Uptake.* Appl Environ Microbiol, 1989. **55**: p. 1735-1741.
35. Stams, A.J. and C.M. Plugge, *Electron transfer in syntrophic communities of anaerobic bacteria and archaea.* Nat Rev Microbiol, 2009. **7**(8): p. 568-77.
36. Abdul Halim, M.F., L.A. Day, and K.C. Costa, *Formate-Dependent Heterodisulfide Reduction in a Methanomicrobiales Archaeon.* Appl Environ Microbiol, 2021. **87**(6).
37. Chowdhury, N.P., et al., *Studies on the mechanism of electron bifurcation catalyzed by electron transferring flavoprotein (Etf) and butyryl-CoA dehydrogenase (Bcd) of Acidaminococcus fermentans.* J Biol Chem, 2014. **289**(8): p. 5145-57.
38. Zheng, Y., et al., *Hydrogen formation and its regulation in Ruminococcus albus: involvement of an electron-bifurcating [FeFe]-hydrogenase, of a non-electron-bifurcating [FeFe]-hydrogenase, and of a putative hydrogen-sensing [FeFe]-hydrogenase.* J Bacteriol, 2014. **196**(22): p. 3840-52.

39. Agne, M., et al., *The missing enzymatic link in syntrophic methane formation from fatty acids.* Proc Natl Acad Sci U S A, 2021. **118**(40).
40. Yitai Liu, D.L.B., Henry C. Aldrich, Gwendolyn R. Drake, David R. Boone, *Characterization of the anaerobic propionate-degrading syntrophs Smithella propionica gen. nov., sp. nov. and Syntrophobacter wolinii.* International Journal of Systematic Bacteriology, 1999. **49**: p. 545-556.
41. de Bok, F.A., et al., *Pathway of propionate oxidation by a syntrophic culture of Smithella propionica and Methanospirillum hungatei.* Appl Environ Microbiol, 2001. **67**(4): p. 1800-4.
42. Sedano-Nunez, V.T., et al., *Comparative proteome analysis of propionate degradation by Syntrophobacter fumaroxidans in pure culture and in coculture with methanogens.* Environ Microbiol, 2018. **20**(5): p. 1842-1856.
43. Hao, L., et al., *Novel syntrophic bacteria in full-scale anaerobic digesters revealed by genome-centric metatranscriptomics.* ISME J, 2020. **14**(4): p. 906-918.
44. Dzofou Ngoumelah, D., et al., *A unified and simple medium for growing model methanogens.* Front Microbiol, 2022. **13**: p. 1046260.
45. Thauer, R.K., *The Wolfe cycle comes full circle.* Proc Natl Acad Sci U S A, 2012. **109**(38): p. 15084-5.
46. Price, M.N., P.S. Dehal, and A.P. Arkin, *FastTree: computing large minimum evolution trees with profiles instead of a distance matrix.* Mol Biol Evol, 2009. **26**(7): p. 1641-50.
47. Chaumeil, P.A., et al., *GTDB-Tk: a toolkit to classify genomes with the Genome Taxonomy Database.* Bioinformatics, 2019.

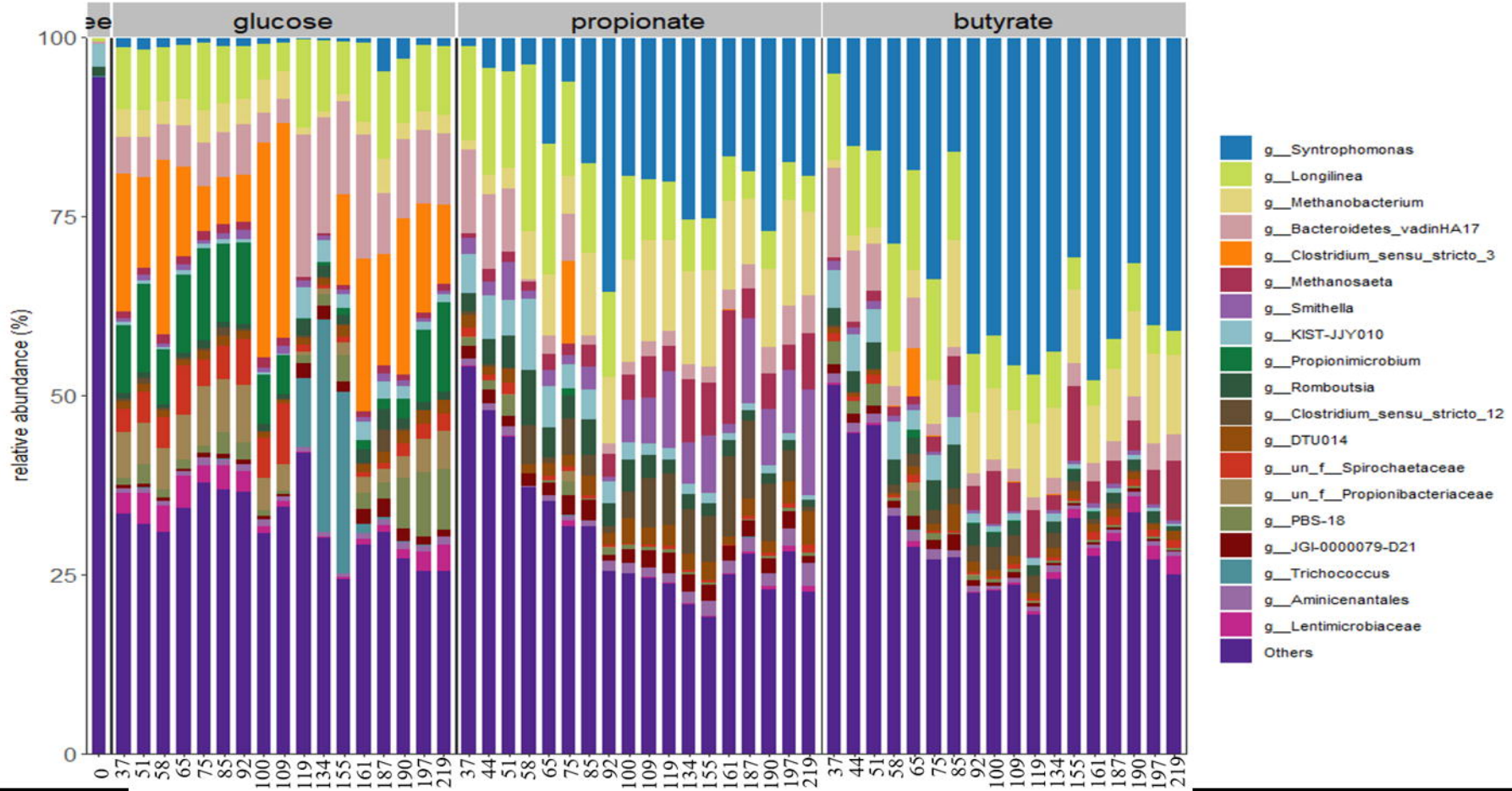
glucose
propionate
butyrate
relative abundance (%)
100
75
50
25
0
g__Syntrophomonas
g__Longilinea
g__Methanobacterium
g__Bacteroidetes_vadinHA17
g__Clostridium_sensu_stricto_3
g__Methanosaeta
g__Smithella
g__KIST-JJY010
g__Propionimicrobium
g__Romboutsia
g__Clostridium_sensu_stricto_12
g__DTU014
g__un_f__Spirochaetaceae
g__un_f__Propionibacteriaceae
g__PBS-18
g__JGI-0000079-D21
g__Trichococcus
g__Aminicenantales
g__Lentimicrobiaceae
Others

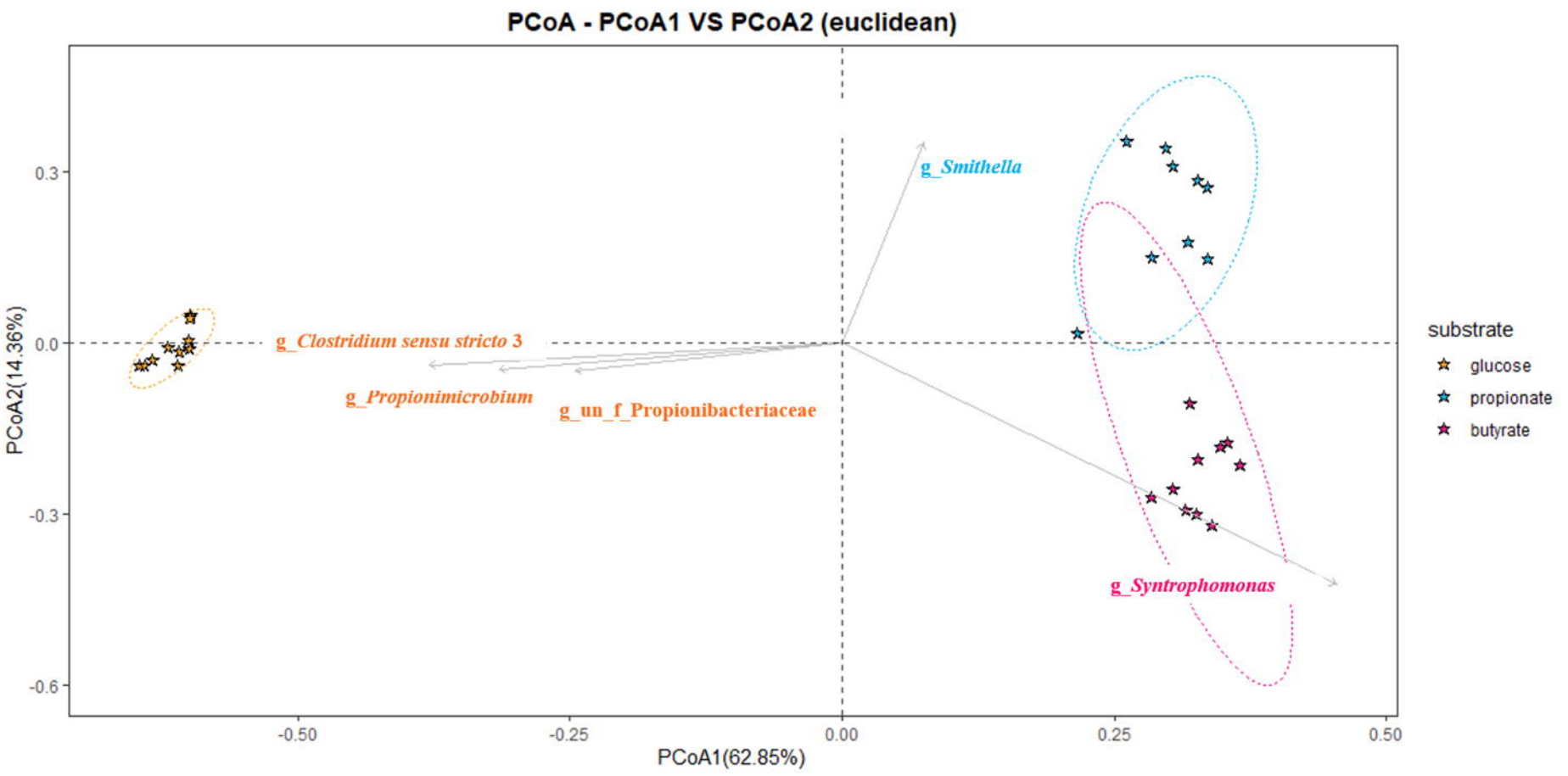
PCoA - PCoA1 VS PCoA2 (euclidean)
g_Smithella
g_Clostridium sensu stricto 3
g_Propionimicrobium
g_un_f_Propionibacteriaceae
g_Syntrophomonas
substrate
glucose
propionate
butyrate
PCoA2(14.36%)
PCoA1(62.85%)
0.3
0.0
-0.3
-0.6
-0.50
-0.25
0.00
0.25
0.50

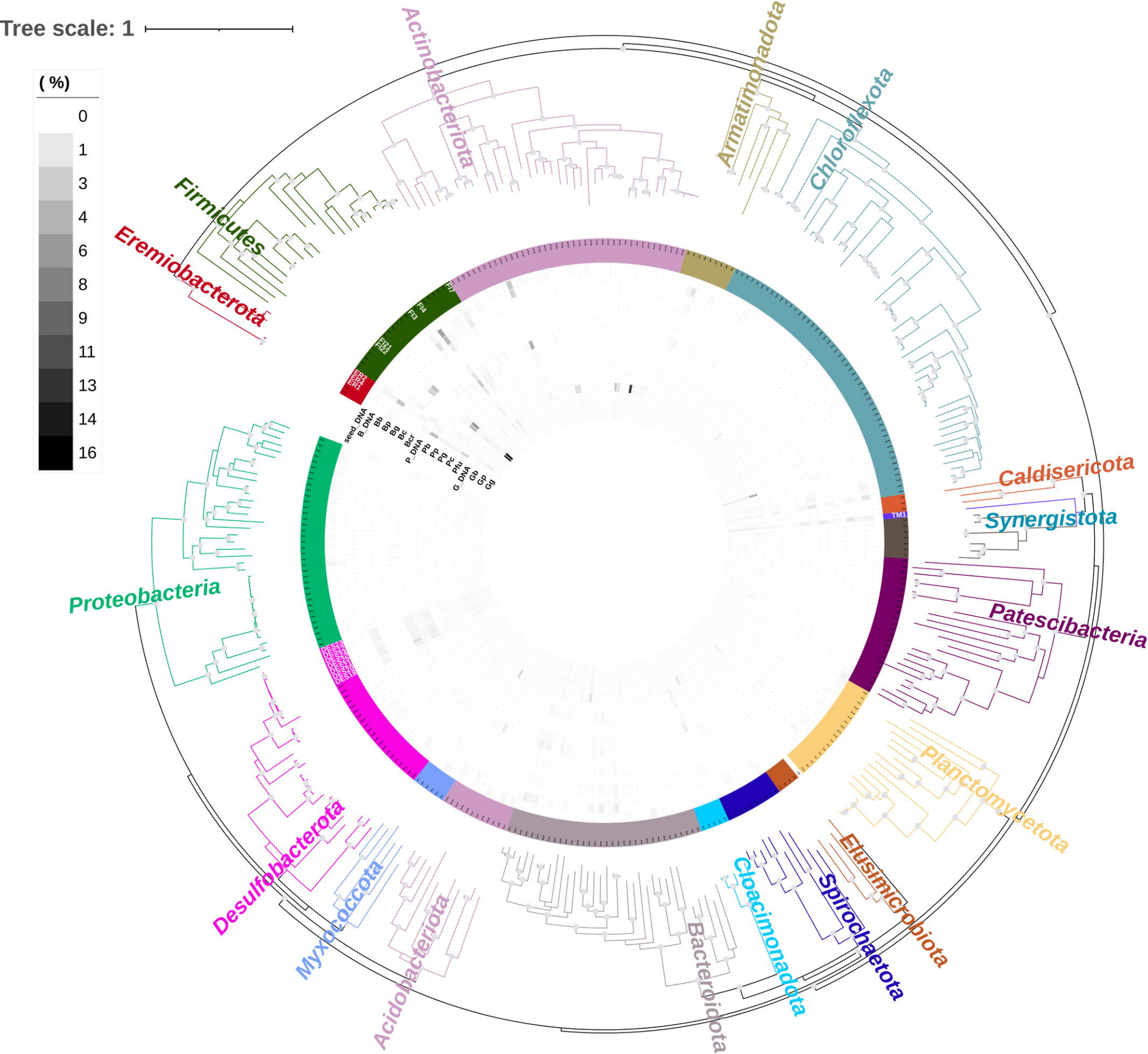

Tree scale: 1
(%)
0
1
3
4
6
8
9
11
13
14
16
Actinobacteriota
Armatimonadota
Chloroflexota
Firmicutes
Eremiobacterota
Caldisericota
Synergistota
Patescibacteria
Proteobacteria
Planctomycetota
Desulfobacterota
Myxococcota
Acidobacteriota
Bacteroidota
Cloacimonadota
Spirochaetota
Elusimicrobiota
seed_DNA
B_DNA
Bb
Bp
Bg
Bc
Bcr
P_DNA
Pb
Pp
Pg
Pc
Pfu
G_DNA
Gb
Gp
Gg
TM1

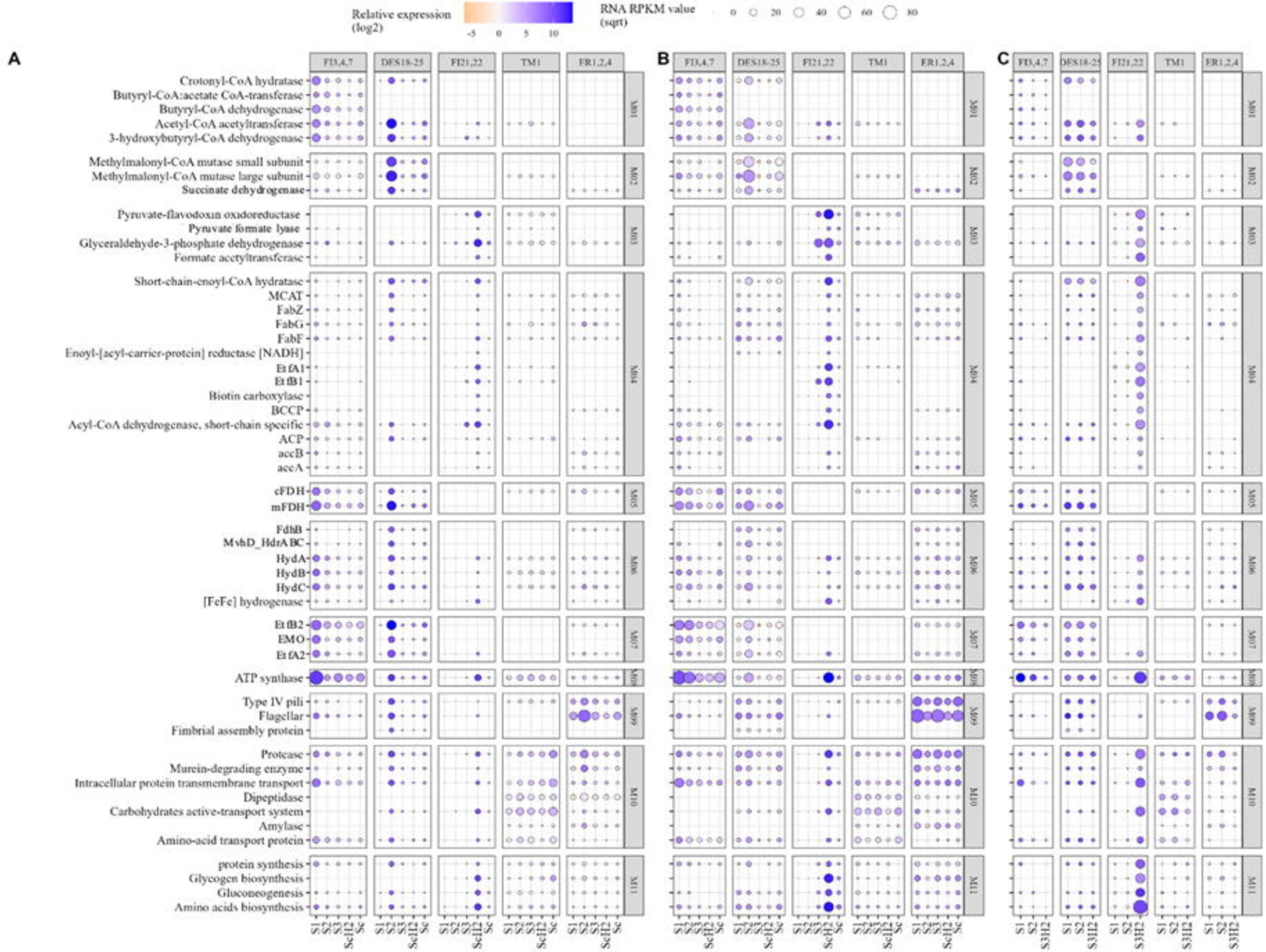

Relative expression (log2)
-5 0 5 10
RNA RPKM value (sqrt)
0 20 40 60 80
A
B
C
FI3,4,7
DES18-25
FI21,22
TM1
ER1,2,4
Crotonyl-CoA hydratase
Butyryl-CoA:acetate CoA-transferase
Butyryl-CoA dehydrogenase
Acetyl-CoA acetyltransferase
3-hydroxybutyryl-CoA dehydrogenase
Methylmalonyl-CoA mutase small subunit
Methylmalonyl-CoA mutase large subunit
Succinate dehydrogenase
Pyruvate-flavodoxin oxidoreductase
Pyruvate formate lyase
Glyceraldehyde-3-phosphate dehydrogenase
Formate acetyltransferase
Short-chain-enoyl-CoA hydratase
MCAT
FabZ
FabG
FabF
Enoyl-[acyl-carrier-protein] reductase [NADH]
EtfA1
EtfB1
Biotin carboxylase
BCCP
Acyl-CoA dehydrogenase, short-chain specific
ACP
accB
accA
cFDH
mFDH
FdhB
MvhD_HdrABC
HydA
HydB
HydC
[FeFe] hydrogenase
EtfB2
EMO
EtfA2
ATP synthase
Type IV pili
Flagellar
Fimbrial assembly protein
Protease
Murein-degrading enzyme
Intracellular protein transmembrane transport
Dipeptidase
Carbohydrates active-transport system
Amylase
Amino-acid transport protein
protein synthesis
Glycogen biosynthesis
Gluconeogenesis
Amino acids biosynthesis
M01
M02
M03
M04
M05
M06
M07
M08
M09
M10
M11
S1 S2 S3 S3H2 Sc

In FBEB-type *hydABC* $4H^+ + Fd_{red} + NADH = 2H_2 + NAD^+ + H^+ + Fd_{ox}$

In *hydABC* gene cluster of SBOB and SPOB $2H^+ + NADH = H_2 + NAD^+ + H^+$

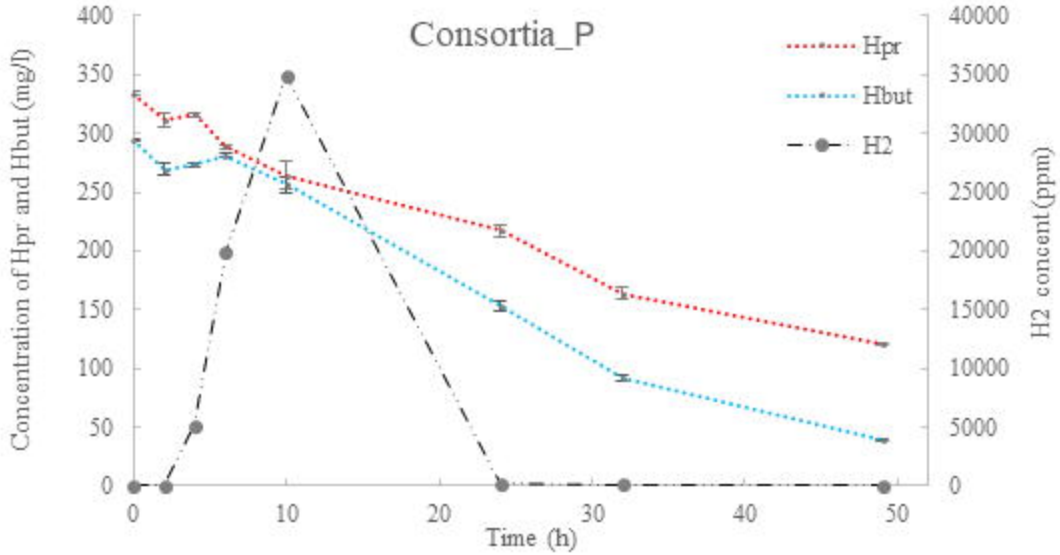

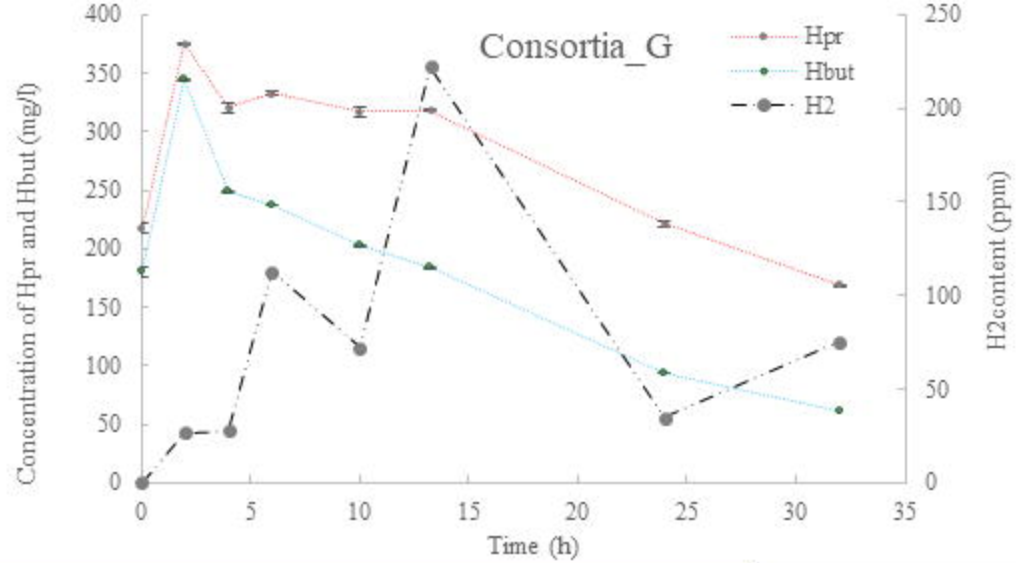

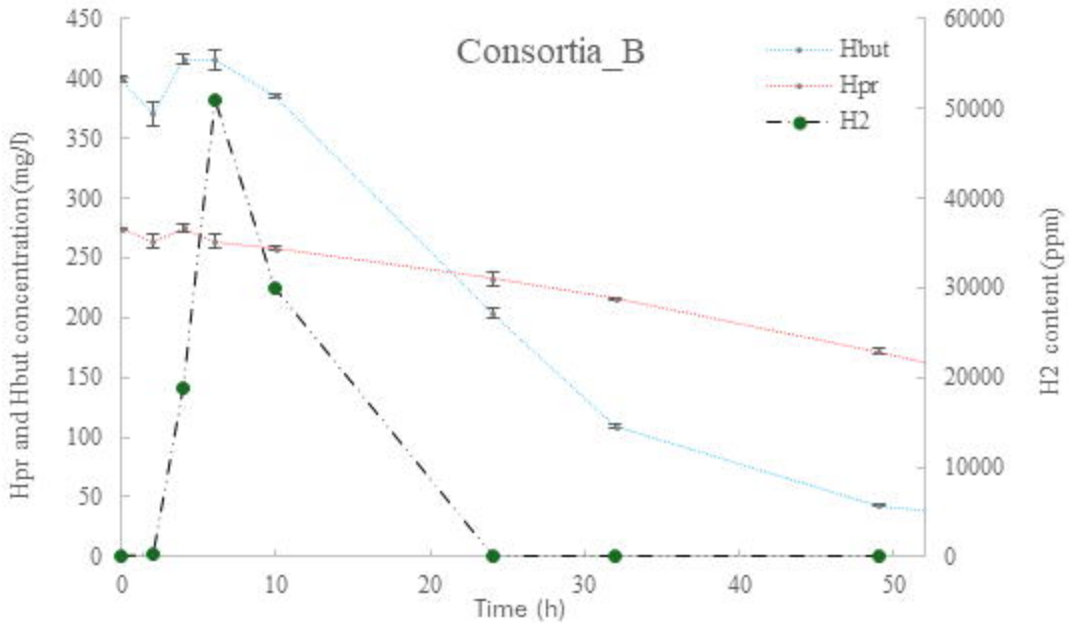

Consortia-P fed with G:B:P=1:1:1						Gibbs free energy change[1] for the acetogenic degradation of		
Time (h)	H_2 (ppm)	Hpr (mg/l)	n-Hbut (mg/l)	HAc (mg/l)	iso-Hbut (mg/l)	Hpr	n-Hbut	iso-Hbut
2	20	312±2	269±2	17±1	9±0.1	-23	-38	-29
4	5114	316±2	273±2	55±0.2	18±0.1	23	50	57
6	19903	289±12	281±7	89±2	20±5	35	73	80
10	34937	264±5	257±5	133±5	24±1	40	81	87
24	174	217±5	153±2	255±8	40±1	2	4	7
32	116	164±1	91±1	248±1	38±0.2	-1	-2	1
49	51	120±1	39±0.3	199±2	34±0.4	-7	-13	-13

Consortia-B fed with G:B:P=1:1:1						Gibbs free energy change for the acetogenic degradation of		
Time (h)	H_2 (ppm)	Hpr (mg/l)	n-Hbut (mg/l)	HAc (mg/l)	iso-Hbut (mg/l)	Hpr	n-Hbut	iso-Hbut
2	353	264±6	399±10	29±0.6	1±0.03	7	16	16
4	18747	275±4	371±4	70±1	34±0.1	71	79	79
6	50975	264±6	416±9	95±2	43±0.3	87	96	96
10	30000	258±1	386±4	101±1	21±0.1	42	50	50
24	103	232±5	203±1	174±5	0	-7	-3	-3
32	107	216±0.4	109±1	182±2	0	-5	-3	-3
49	51	172±2	43±4	91±1	0	-16	-16	-16

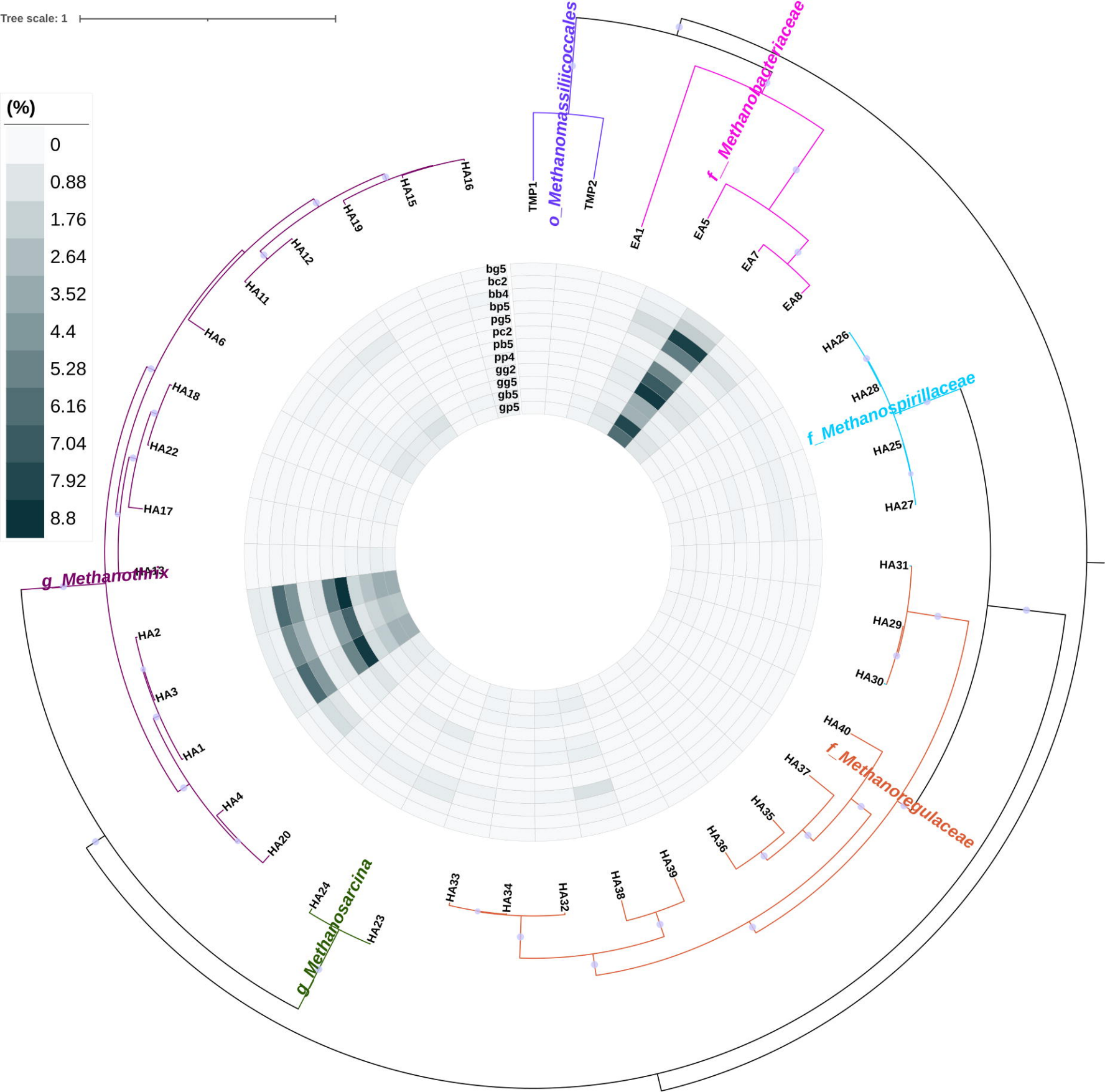
Tree scale: 1
(%)
0
0.88
1.76
2.64
3.52
4.4
5.28
6.16
7.04
7.92
8.8
o_Methanomassiliicoccales
f_Methanobacteriaceae
f_Methanospirillaceae
f_Methanoregulaceae
g_Methanothrix
g_Methanosarcina
TMP1
TMP2
EA1
EA5
EA7
EA8
HA16
HA15
HA19
HA12
HA11
HA6
HA18
HA22
HA17
HA13
HA2
HA3
HA1
HA4
HA20
HA24
HA23
HA33
HA34
HA32
HA38
HA39
HA36
HA35
HA37
HA40
HA30
HA29
HA31
HA27
HA25
HA28
HA26
bg5
bc2
bb4
bp5
pg5
pc2
pb5
pp4
gg2
gg5
gb5
gp5

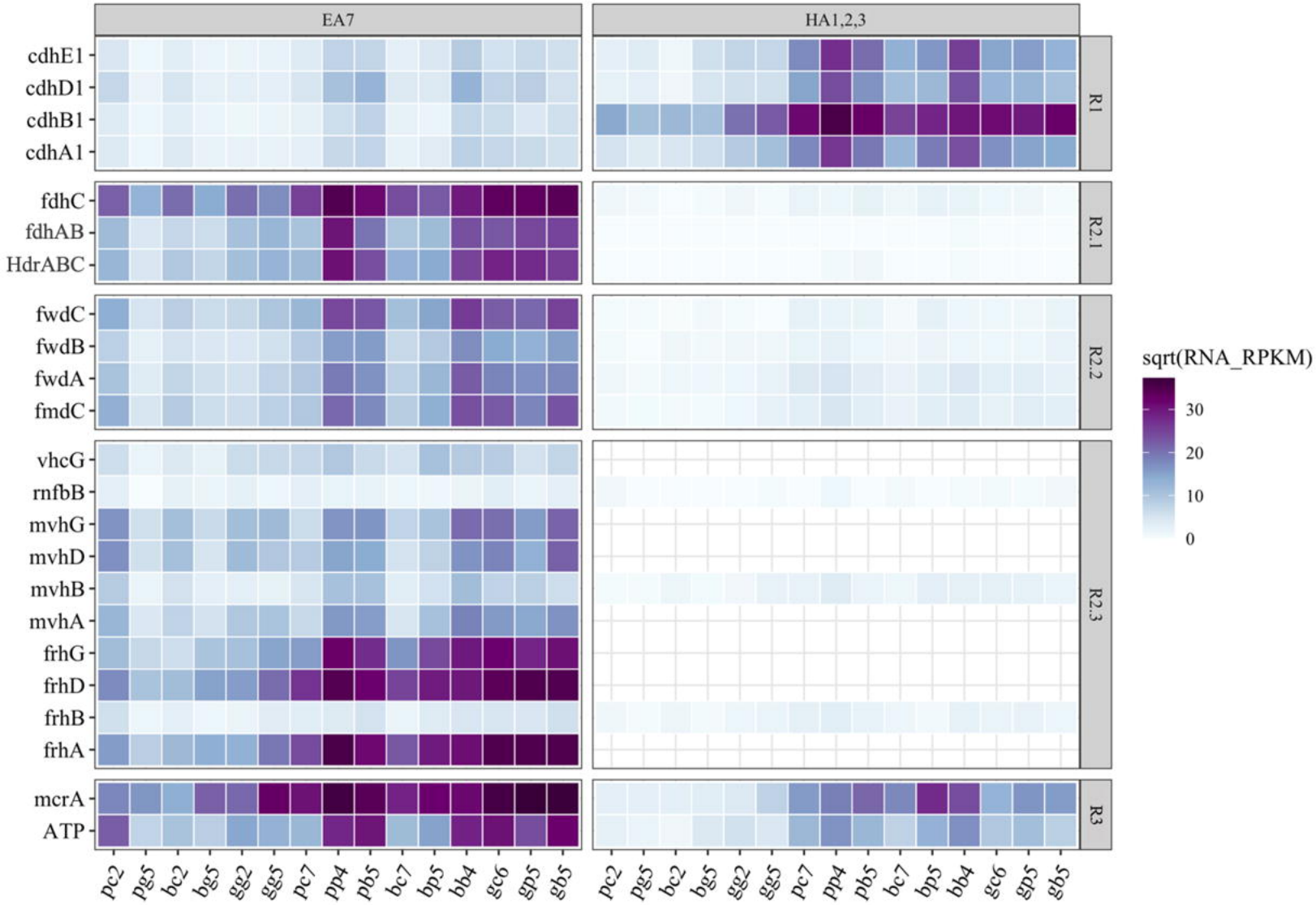
EA7
HA1,2,3
cdhE1
cdhD1
cdhB1
cdhA1
fdhC
fdhAB
HdrABC
fwdC
fwdB
fwdA
fmdC
vhcG
rnfbB
mvhG
mvhD
mvhB
mvhA
frhG
frhD
frhB
frhA
mcrA
ATP
R1
R2.1
R2.2
R2.3
R3
pc2
pg5
bc2
bg5
gg2
gg5
pc7
pp4
pb5
bc7
bp5
bb4
gc6
gp5
gb5
sqrt(RNA_RPKM)
30
20
10
0

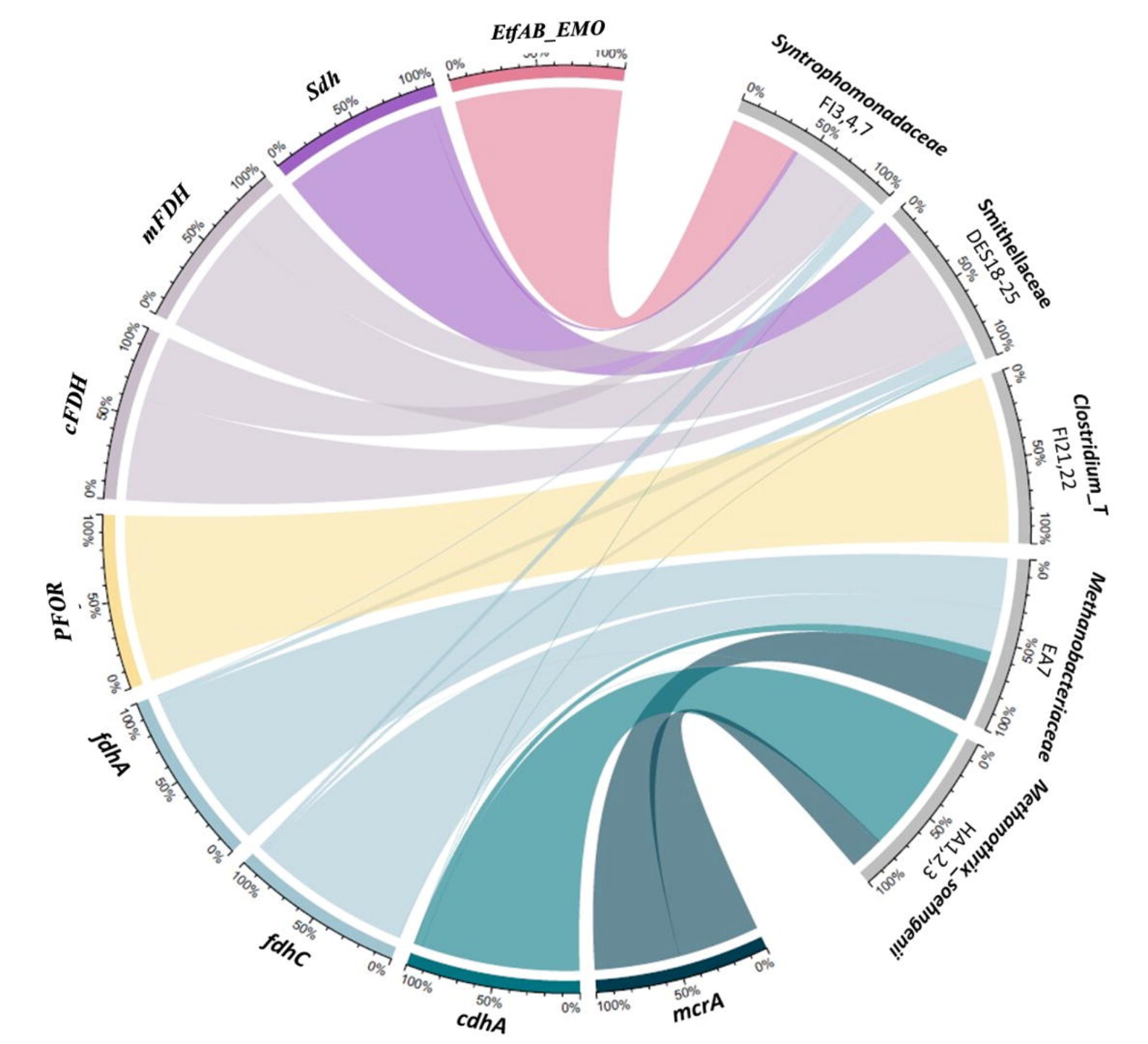
EtfAB_EMO
Syntrophomonadaceae
FI3,4,7
Smithellaceae
DES18-25
Clostridium_T
FI21,22
Methanobacteriaceae
EA7
Methanothrix_soehngenii
HA1,2,3
mcrA
cdhA
fdhC
fdhA
PFOR
cFDH
mFDH
Sdh
0%
50%
100%